Limnol. Oceanogr., 58(2), 2013, 475–488

doi:10.4319/lo.2013.58.2.0475

Groundwater-derived dissolved inorganic and organic carbon exports from a mangrove tidal creek: The missing mangrove carbon sink?

D. T. Maher,* I. R. Santos, L. Golsby-Smith, J. Gleeson, and B. D. Eyre

Centre for Coastal Biogeochemistry, School of Environment, Science and Engineering, Southern Cross University, Lismore, New South Wales, Australia

Abstract

A majority of the global net primary production of mangroves is unaccounted for by current carbon budgets. It has been hypothesized that this ''missing carbon'' is exported as dissolved inorganic carbon (DIC) from subsurface respiration and groundwater (or pore-water) exchange driven by tidal pumping. We tested this hypothesis by measuring concentrations and $\delta^{13}C$ values of DIC, dissolved organic carbon (DOC), and particulate organic carbon (POC), along with radon (^{222}Rn, a natural submarine groundwater discharge tracer), in a tidal creek in Moreton Bay, Australia. Concentrations and $\delta^{13}C$ values displayed consistent tidal variations, and mirrored the trend in ^{222}Rn in summer and winter. DIC and DOC were exported from, and POC was imported to, the mangroves during all tidal cycles. The exported DOC had a similar $\delta^{13}C$ value in summer and winter ($\sim -30‰$). The exported $\delta^{13}C$-DIC showed no difference between summer and winter and had a $\delta^{13}C$ value slightly more enriched ($\sim -22.5‰$) than the exported DOC. The imported POC had differing values in summer ($\sim -16‰$) and winter ($\sim -22‰$), reflecting a combination of seagrass and estuarine particulate organic matter (POM) in summer and most likely a dominance of estuarine POM in winter. A coupled ^{222}Rn and carbon model showed that 93–99% of the DIC and 89–92% of the DOC exports were driven by groundwater advection. DIC export averaged 3 g C m^{-2} d^{-1} and was an order of magnitude higher than DOC export, and similar to global estimates of the mangrove missing carbon (i.e., $\sim$ 1.9–2.7 g C m^{-2} d^{-1}).

The link between terrestrial and marine carbon cycles is an important yet poorly constrained component of the global carbon cycle. Most models of the global carbon cycle only include three reservoirs (terrestrial, marine, and atmosphere) with the link between terrestrial and marine components defined as an ''unreactive pipe'' (Cole et al. 2007). This unreactive pipe is defined as the flow of terrestrial-derived organic matter via surface waters (i.e., rivers) to the ocean. However, studies suggest that significant transformations of the organic matter pool occur during transport (Peterson et al. 1994; Maher and Eyre 2010), and that there is a substantial, yet poorly constrained, flow of terrestrial carbon through subsurface pathways (Cai et al. 2003; Santos et al. 2009). In addition, our understanding of the transport and transformation of carbon as it transits from terrestrial to oceanic biomes suffers from a lack of data from a variety of ecosystems and latitudes, including mangroves (Bouillon et al. 2008; Kristensen et al. 2008*a*; Alongi 2009).

Mangroves are a dominant habitat in tropical and subtropical coastal areas, and exert a strong control over carbon cycling at a local, regional, and global scale. Mangroves contribute up to $\sim$ 10% of the global terrestrially derived particulate organic carbon (POC; Jennerjahn and Ittekkot 2002) and dissolved organic carbon (DOC; Dittmar et al. 2006) exported to the coastal zone. Further, mangrove forests are among the most carbon-rich tropical forests, with a majority of the carbon belowground (Donato et al. 2011). In spite of the clear importance of these ecosystems in terms of the global carbon cycle, more than half of the carbon fixed by mangroves (112–160 Tg C yr^{-1}) is unaccounted for by estimates of the various carbon sinks (Bouillon et al. 2008; Alongi 2009). This may represent a large global flux of carbon equivalent to $\sim$ 12–17% of the ''missing anthropogenic carbon sink.'' Bouillon et al. (2008) suggested that mineralization rates may be significantly underestimated because of the methods used (e.g., diffusive core incubations) and much of the missing carbon may be exported as dissolved inorganic carbon (DIC) through tidal exchange and/or directly lost to the atmosphere as CO_2 gas. Indeed, mineralization rates based on diffusive fluxes across the sediment–water interface may significantly underestimate depth integrated rates in mangroves (Alongi et al. 2012), and much of the DIC produced may be exported via subsurface advective exchange associated with tidal pumping.

Evidence that advective transport of groundwater (or pore water) enriched in DIC and DOC may be a dominant pathway for carbon export from mangroves has been shown by several studies. For example, Bouillon et al. (2007*b*) estimated that pore water contributed between 19% and 87% of a Tanzanian mangrove creek's volume at low tide based on DOC, salinity, and dissolved oxygen concentrations. Koné and Borges (2008) concluded that pore-water DIC, derived from anaerobic organic matter degradation through the sulfate reduction pathway, was a significant contributor to the total DIC pool based on alkalinity and DIC stoichiometry. Dittmar and Lara (2001) suggested that pore-water flow is probably a major driver of nutrients and DOC in a Brazilian mangrove tidal creek. However, direct measurements quantifying the groundwater-derived DIC export from mangroves have not been reported. Further, there are few quantitative measurements

* Corresponding author: damien.maher@scu.edu.au

of DIC export from mangroves (Miyajima et al. 2009), and to our knowledge, no studies have compared the relative contribution of DIC, DOC, and POC to total carbon exchange from mangrove systems.

Groundwater inputs to receiving waterways have traditionally been difficult to quantify, especially in heterogeneous coastal sediments (Burnett et al. 2006). Radon (^{222}Rn) is an excellent natural groundwater tracer because of its conservative nature and the high concentrations in groundwater relative to surface water. ^{222}Rn has been used successfully to trace groundwater inputs in lakes (Schmidt et al. 2010), rivers (Cook et al. 2006), estuaries (Charette and Buesseler 2004; Santos et al. 2012*a*), coral reefs (Cardenas et al. 2010), and the coastal ocean (Burnett et al. 2006). The large range of systems where ^{222}Rn has been used to trace groundwater highlights the utility of this tracer. Recent technological advances (i.e., automation) have led to an increased use of ^{222}Rn as a groundwater tracer (Burnett et al. 2010). Qualitative ^{222}Rn surveys along coastal areas of the Great Barrier Reef surrounded by mangrove forests have indicated that mangroves may be regional hotspots (Stieglitz et al. 2010), but groundwater exchange rates have not been quantified.

We hypothesized that DIC makes a significant contribution to the total carbon export from mangrove ecosystems, and that this export is driven by DIC sourced from groundwater exchanged by advective tidal pumping rather than diffusive flux. We have tested these hypotheses by performing time series measurements of ^{222}Rn and key carbon chemistry parameters in a tidal creek with no upstream freshwater inputs. Tidal pumping is related to seawater infiltration into beach and bank sediments at high tide and pore-water discharge at low tide (Robinson et al. 2007). Previous modeling investigations have advanced our understanding of tidal pumping in coastal mangrove wetlands (Mazda and Ikeda 2006; Yuan et al. 2011) but a quantitative link between tidal pumping in mangrove sediments and carbon cycling has not yet been established.

Methods

Study area—The study was conducted in a small, well-defined mangrove creek with no upstream freshwater input, located in the subtropical southern Moreton Bay, on the east coast of Australia (Fig. 1). The same creek was used previously for nitrogen and phosphorus exports in Eyre et al. (2011*a*). The tidal regime is semidiurnal with neap tide and spring tide ranges of ~ 1 and 2 m, respectively. The dominant mangrove species are *Avicennia marina*, *Aegiceras corniculatum, Bruguiera gymnorrhiza,* and *Rhizophora stylosa*, with smaller isolated populations of *Ceriops australis, Excoecaria agallocha*, and *Lumnitzera racemosa*. Crab burrows are the predominant feature of the sediments, and the fiddler crabs species that are dominant in the area (*Uca vocans and Uca bellator minima*; Meziane et al. 2006) are known to create new burrows after each tidal cycle (Lim 2006). Sampling campaigns were conducted in winter (July 2011) and summer (January 2012) during spring tides (maximum tidal amplitude ~ 2 m).

Time series—Samples for pH and DIC, DOC, and POC concentration and stable isotope ratios were collected from near the mouth of the creek from a depth of ~ 10 cm (27°46′48.9″S, 153°22′51.1″E; Fig. 1) every hour over a 27 and 30 h time series in winter and summer, respectively. Samples for DIC and DOC were collected with a sample-rinsed polypropylene syringe and filtered through Whatman GF/F filters into acid-rinsed precombusted (450°C for 4 h) 40 mL volatile organic carbon (VOC) borosilicate vials containing 100 μL of saturated $HgCl_2$ solution, leaving no headspace or bubbles. In winter, samples for POC were collected in 1 liter polypropylene bottles and kept at 4°C until returning to the lab, where they were filtered through precombusted GF/F filters within 4 days from collection. During summer, POC samples were immediately filtered upon collection through precombusted GF/F filters and kept at −20°C until analysis. Prior to analysis, POC filters were fumed with concentrated HCl for 24 h, then dried at 60°C for 24 h to remove any inorganic carbon. pH (± 0.005 units) was determined using a Metrohm 826, and wind speed was measured hourly at a height of 3 m using a handheld anemometer. ^{222}Rn was measured using an automated ^{222}Rn-in-air analyzer (RAD7, Durridge) and a showerhead air–water exchanger following Santos et al. (2012*b*).

Groundwater—Groundwater was collected during low tide along a transect from just above the low tide level to the high tide level (n = 4 sites) by digging bores to a depth of ~ 30 cm below the water table. The water in each bore was purged at least two times, and samples for DIC and DOC were collected by syringe from near the bottom of the bore as the water recharged, and treated as described earlier. ^{222}Rn samples were collected using 250 mL gas bottles and analyzed with the RAD7's Rad-H_2O system (Dulaiova et al. 2005).

Diffusive flux—Sediment cores were collected from the lower (n = 3) and upper (n = 3) intertidal areas within the mangroves to determine diffusive DIC and DOC fluxes during summer. Cores were incubated under mean daily in situ irradiance and temperatures over a diel cycle, in the laboratory, with samples for DIC and DOC collected at dusk, dawn, and dusk (for full details on incubation methodology *see* Maher and Eyre 2011*a*). An additional three "blank" cores containing only site water were incubated to correct for concentration changes associated with water column processes. Fluxes were calculated using

$$F = ([C_{t1} - C_{t0}] \times V/SA)T \quad (1)$$

where F = flux rate (μmol m^{-2} h^{-1}); C_{t1} = concentration of DIC or DOC at the end of the incubation period (μmol C L^{-1}); C_{t0} is the initial DIC or DOC concentration (μmol C L^{-1}); V is the volume of overlying water (L); SA is the sediment surface area (m^2); and T is the incubation time (h). Dark fluxes are based on concentration change during the dark period, light fluxes are based on changes during the light, and net fluxes are based on dark and light fluxes, accounting for the hours of daylight and nighttime during each season.

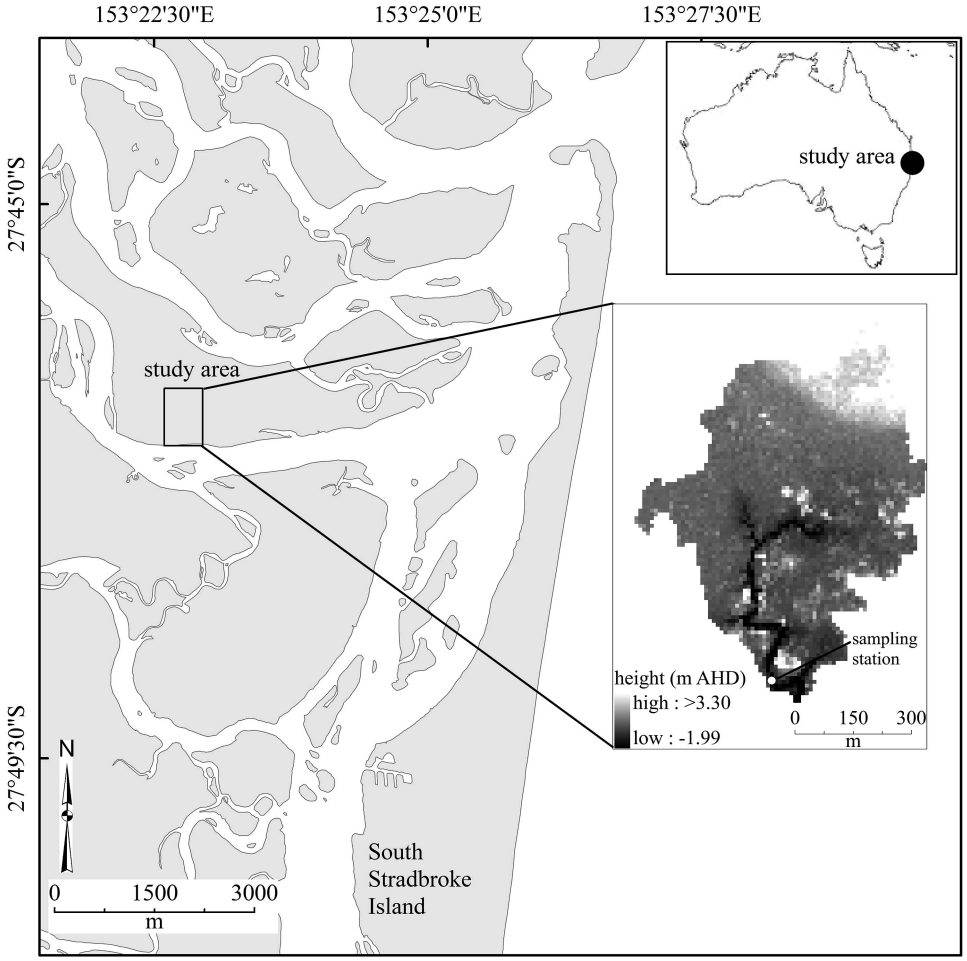

Fig. 1. Map of study area, including the DEM of the study creek. Heights are meters AHD. Groundwater samples were taken adjacent to the sampling station.

End-member isotopes—Samples of the primary producer end members for the mangrove forest and adjacent estuary were collected during winter for carbon stable isotope analysis. In total nine different end members were collected: estuarine particulate organic matter (POM; used as a proxy for phytoplankton), fresh *A. marina* and *R. stylosa* leaves, mangrove litterfall (mixed), fresh *Sporobolus virginicus* leaves (the dominant saltmarsh species), mangrove fruit (mixed), pneumatophore-attached macroalgae, *Zostera capricorni* leaves (from the adjacent estuary), and benthic microalgae from within the mangroves. The estuarine POM samples were collected by filtering ~ 1 liter of estuarine water collected at high tide through a precombusted GF/F filter, ensuring no large debris contaminated the sample. Benthic microalgae samples were collected by scraping the top 1 mm of the sediment surface where a visible patch of microalgae was present, ensuring no large debris was retained. All other samples were collected by hand, and all samples were placed into tin foil and frozen prior to analysis (within 2 weeks). Samples were dried (60°C), ground to a fine powder using mortar and pestle, and fumed with concentrated HCl for 24 h, then dried at 60°C for 24 h to remove any inorganic carbon. Triplicate samples of each end member were analyzed.

Analysis—DIC and DOC samples were analyzed for concentration and carbon stable isotope ratios using the wet-oxidation method (St-Jean 2003) using an OI Aurora 1030W interfaced with a Thermo Delta V+ Isotope Ratio Mass Spectrometer (IRMS) (Maher and Eyre 2011*b*). POC, primary producer end-member carbon concentration, and carbon stable isotope ratios were measured using a Flash EA coupled to a Thermo Delta V+ IRMS via a continuous flow interface. All stable carbon isotope ratios were calculated relative to the international standard (PDB). Reproducibility of δ^{13}C-DIC, -DOC, and -POC measurements was $< 0.3‰$, $<0.5‰$, and $<0.2‰$, respectively. The coefficients of variation between triplicate measurements for DIC, DOC, and POC concentrations were $< 0.5\%$, $< 2\%$, and $< 0.2\%$, respectively.

Modeling—To quantify the relative importance of subsurface exchange of DIC and DOC in the total carbon export we used a combined ^{222}Rn, DIC, and DOC mixing model. ^{222}Rn concentration in the creek was used as a first-order estimate for volumetric groundwater input using the following equation (Peterson et al. 2010):

$$f_{gw} = (Rn_m - Rn_{imp})/Rn_{gw} \quad (2)$$

where f_{gw} is fraction of groundwater within the creek, Rn_m is the measured ^{222}Rn concentration in the creek water, Rn_{imp} is the ^{222}Rn concentration of the imported water (i.e., the high tide ^{222}Rn concentration) and Rn_{gw} is the measured groundwater ^{222}Rn concentration. Rn_m is corrected for the air–water Rn flux using creek volumes and a mass balance. DIC concentration was then modeled assuming that groundwater was the sole pathway for DIC input using the following equation:

$$DIC_{modeled} = (f_{gw} \times DIC_{gw}) + [(1 - f_{gw}) \times DIC_{imp}] \quad (3)$$

where $DIC_{modeled}$ is the modeled DIC concentration, DIC_{gw} is the groundwater DIC concentration, and DIC_{imp} is the DIC concentration of the imported water (i.e., high tide DIC concentration). DIC_{gw} displayed a linear relationship with height above low tide (*see* Results), and this relationship was used to estimate DIC_{gw} at each hourly interval based on measured water height. The same model was used to model groundwater-derived DOC input; however, there was no significant relationship between height above low tide and DOC concentration; therefore, we used the average of the measured groundwater concentrations.

To compare modeled and measured concentrations of DIC, a correction must be made for the air–water flux of CO_2, as this is not accounted for by the model. The measured DIC concentration was corrected for the air–water CO_2 flux by

$$DIC_{corrected} = [(CO_{2\,flux} \times SA) + (DIC_m \times Vol)]/Vol \quad (4)$$

where $DIC_{corrected}$ is the corrected DIC concentration, $CO_{2\,flux}$ is the air water CO_2 flux (μmol C m^{-2} h^{-1}), SA is the surface area of the water in the creek, DIC_m is the measured DIC concentration (μmol C L^{-1}) and Vol is the volume of the creek.

The partial pressure of CO_2 (PCO_2) within the creek was determined by DIC and pH using the CO2SYS program (Lewis and Wallace 1998) with the carbonic acid disassociation constants from Millero et al (2006) and the $KHSO_4$ from Dickson (1990). The air–water CO_2 flux within the mangrove creek was estimated at hourly intervals assuming homogenous PCO_2 and wind speed within the creek water and an atmospheric CO_2 concentration of 38.5 Pa using the wind speed transfer velocity parameterization of Raymond and Cole (2001), correcting for the Schmidt number of CO_2 at in situ temperature and salinity (Wanninkhof 1992). Wind speed was measured at a height of 3 m (U_3) and was converted to the speed at 10 m (U_{10}) using the power law assuming a roughness exponent of 0.143 (Robeson and Shein 1997). The flux of ^{222}Rn from the creek to the atmosphere was calculated assuming homogenous concentration and wind speed within the creek, using the wind speed transfer velocity parameterization of Wanninkhof (1992) with concentrations corrected for the Schmidt number of ^{222}Rn at in situ temperature and salinity (Wanninkhof 1992).

A stable isotope ratio mass balance model was also used to determine groundwater-derived inputs of DIC and DOC to the creek water, using the following equation:

$$\delta^{13}C\text{-}DIC_{modeled} = [(f_{gw} \times DIC_{gw} \times \delta^{13}C\text{-}DIC_{gw}) + ((1 - f_{gw}) \times DIC_{imp} \times \delta^{13}C\text{-}DIC_{imp})]/DIC_m \quad (5)$$

were $\delta^{13}C$-$DIC_{modeled}$ is the modeled DIC carbon stable isotope ratio, $\delta^{13}C$-DIC_{gw} is the groundwater DIC carbon stable isotope ratio, DIC_m is the measured DIC concentration, and $\delta^{13}C$-DIC_{imp} is the DIC carbon stable isotope ratio of the imported water (i.e., the high tide concentration). DIC_m was corrected for the air–water CO_2 flux, and for comparison between modeled and measured $\delta^{13}C$-DIC the measured $\delta^{13}C$-DIC was corrected for the fractionation of the DIC pool associated with the air–water flux of CO_2 using the linear function of ε_d and temperature described by Zhang et al. (1995) and the mole fractions of $CO_{2(aq)}$, HCO_3, and CO_3^{2-} (calculated using CO2SYS). An isotope mass balance was used to correct for ε_d associated with the air–water CO_2 flux:

$$\delta^{13}C\text{-}DIC_{corrected} = [((DIC_{corrected} - DIC_m) \times (\delta^{13}C\text{-}DIC_m - \varepsilon_d)) + (DIC_m \times \delta^{13}C\text{-}DIC_m)] / DIC_{corrected} \quad (6)$$

where $\delta^{13}C$-$DIC_{corrected}$ is the stable carbon isotope value of DIC in the creek, corrected for the fractionation of the DIC pool associated with air–water CO_2 flux; $\delta^{13}C$-DIC_m is the measured stable carbon isotope value of DIC in the creek; and ε_d is the fractionation factor for DIC because of the air–water CO_2 flux at in situ temperature and DIC molar fractions and a salinity of 35 (Zhang et al. 1995).

Carbon exchange—A digital elevation model (DEM; 10 m grid size, elevation accuracy ± 0.2 m) of the catchment was constructed using data from Airborne Laser Survey (for areas > 0 m Australian Height Datum [AHD]) and hydrological surveys (for areas < 0 m AHD). The DEM was used to delineate the catchment boundary using the ArcMap Hydrology toolbox. Four Van Essen conductivity, temperature, depth (CTD) divers were deployed within the channel of the creek, spaced roughly equidistantly from the mouth to the uppermost section that was still inundated at low tide. A CTD diver was also deployed within the adjacent estuary. Water volume within the catchment throughout the study was determined at 10 min intervals using the DEM and CTD diver data for each section of the creek and the ArcMap 3D Analyst toolbox, and from this, hourly water fluxes were derived.

Export and import of individual forms of carbon (DIC, DOC, and POC) were calculated based on the regression method of Boto and Wellington (1988), with the exception that a power relationship, not a linear relationship, between creek volume and concentration was established. The flux was calculated as the difference in the integrated area below the regression for each flood and ebb tide cycle. Where regressions were not significant ($p > 0.05$), a one-way

Table 1. Composition of intertidal groundwater within the mangrove forest during the study. All samples were taken from ~ 30 cm below the water table from hand-augured bores along a transect starting at the low tide mark. nd, not determined.

	Sediment height (m AHD)	DIC concentration (μmol C L^{-1})	δ^{13}C-DIC (‰)	DOC concentration (μmol C L^{-1})	δ^{13}C-DOC (‰)	^{222}Rn concentration (Bq m^{-3})
Summer						
Bore 1	1.1	6426	−14.5	235	−24.57	458
Bore 2	1.3	6075	−13.7	261	−24.25	nd
Bore 3	1.4	5092	−12.8	225	−24.81	943
Bore 4	1.7	4713	−12.3	258	−25.17	705
Winter						
Bore 1	0.9	5479	−13.2	234	−23.28	573
Bore 2	1.2	5284	−12.8	580	−24.04	908
Bore 3	1.4	4340	−11.6	345	−23.40	nd
Bore 4	2.3	3767	−10.0	812	−24.12	833

analysis of variance was carried out to test for significant difference in concentrations between ebb and flood tide. If a significant difference was found, the mean concentration was integrated over the appropriate volume to determine the flux (Boto and Wellington 1988); if no significant difference was found it is assumed that the net flux was not significantly different from zero. A regression method was also used to quantify the relative magnitude of the groundwater-derived vs. total DIC and DOC flux. The difference between the integration of measured and modeled regressions during ebb tides was defined as the non-groundwater component of the carbon export.

Results

Groundwater—Groundwater concentrations of DIC were high, ranging from 3767 to 6426 μmol C L^{-1} throughout the study, with a trend of increasing concentration with decreasing elevation (Table 1). DOC concentrations showed an opposite trend to DIC during winter, with decreasing concentrations with decreasing elevation, ranging from 200 to 800 μmol C L^{-1}. DOC concentrations during summer were similar along the transect, ranging from 220 to 260 μmol C L^{-1} (Table 1). Groundwater ^{222}Rn concentrations ranged from ~ 458 to 953 Bq m^{-3} throughout the study, with no clear seasonal or spatial trends. δ^{13}C-DOC values displayed a small variation throughout the study, ranging from −25.2‰ to −23.2‰ (Table 1). δ^{13}C-DIC values displayed enrichment from low to high elevation during both summer and winter, with values ranging from −14.5‰ to −10.0‰.

Tidal creek time series—There was a clear tidal trend for most measured parameters during summer and winter, with the highest concentrations of DIC, DOC, POC, and ^{222}Rn occurring at low tide and the lowest concentrations occurring at high tide (Fig. 2). The concentration range for each parameter was similar between winter and summer, with DIC ranging from 2064 to 2800 μmol C L^{-1}, DOC from 80 to 200 μmol C L^{-1}, POC from 30 to 550 μmol C L^{-1}, and ^{222}Rn from ~ 20 to 242 Bq m^{-3}.

Values of δ^{13}C-DIC ranged between −5.5‰ and +2.3‰ in the creek throughout the study and δ^{13}C-DOC values ranged from ~ −24.3‰ to −13.1‰ (Fig. 3). The δ^{13}C-DIC and δ^{13}C-DOC values showed a clear tidal trend, with enriched values at high tide and more depleted values during low tide (Fig. 3). δ^{13}C-POC values ranged from −27.8‰ to −12.8‰ during the study, and there was a trend of more enriched values just prior to low tide during summer and no discernible tidal trend during winter (Fig. 3).

Diffusive sediment flux—The diffusive sediment–water DIC fluxes were slightly higher for the high intertidal area than the low intertidal area. These core incubations indicated that the sediments were a net source of DIC over a diel cycle (Table 2). Fluxes were only slightly lower during the light, indicating low rates of benthic productivity.

End-member analysis—The primary producer end members displayed significant variation. The δ^{13}C of mangroves ranged from ~ −27.6‰ ± 0.5‰ (*R. stylosa* leaves) to −24.5‰ ± 0.5‰ (mixed mangrove litter). Seagrass (*Z. capricorni*) and saltmarsh (*S. virginicus*) δ^{13}C values were similar (−12.6‰ ± 0.4‰ and −12.8‰ ± 0.7‰, respectively) and benthic microalgae, estuarine POM, and pneumatophore macroalgae were −18.2‰ ± 0.9‰, −21.5‰ ± 2.1‰, and −22.8‰ ± 0.6‰, respectively.

Modeling—Modeled concentrations of DIC and DOC agreed well with measured concentrations during both summer and winter (Fig. 4). The greatest differences between modeled and measured concentrations of DIC and DOC occurred at low tide. The modeled δ^{13}C-DIC values followed the corrected measured δ^{13}C-DIC values throughout the tidal cycle during both summer and winter. The modeled δ^{13}C-DOC followed the same trend as the measured values; however, modeled values were not as depleted as measured values during low tide.

Carbon export—DIC made the largest contribution to carbon export from the mangrove system during all tidal cycles, ranging from 7626 to 14,169 μmol C m^{-2} h^{-1} (Fig. 5). POC was consistently imported to the mangrove during each tidal cycle, with the largest import rate occurring during the summer large tide (3980 μmol C m^{-2} h^{-1}). DOC

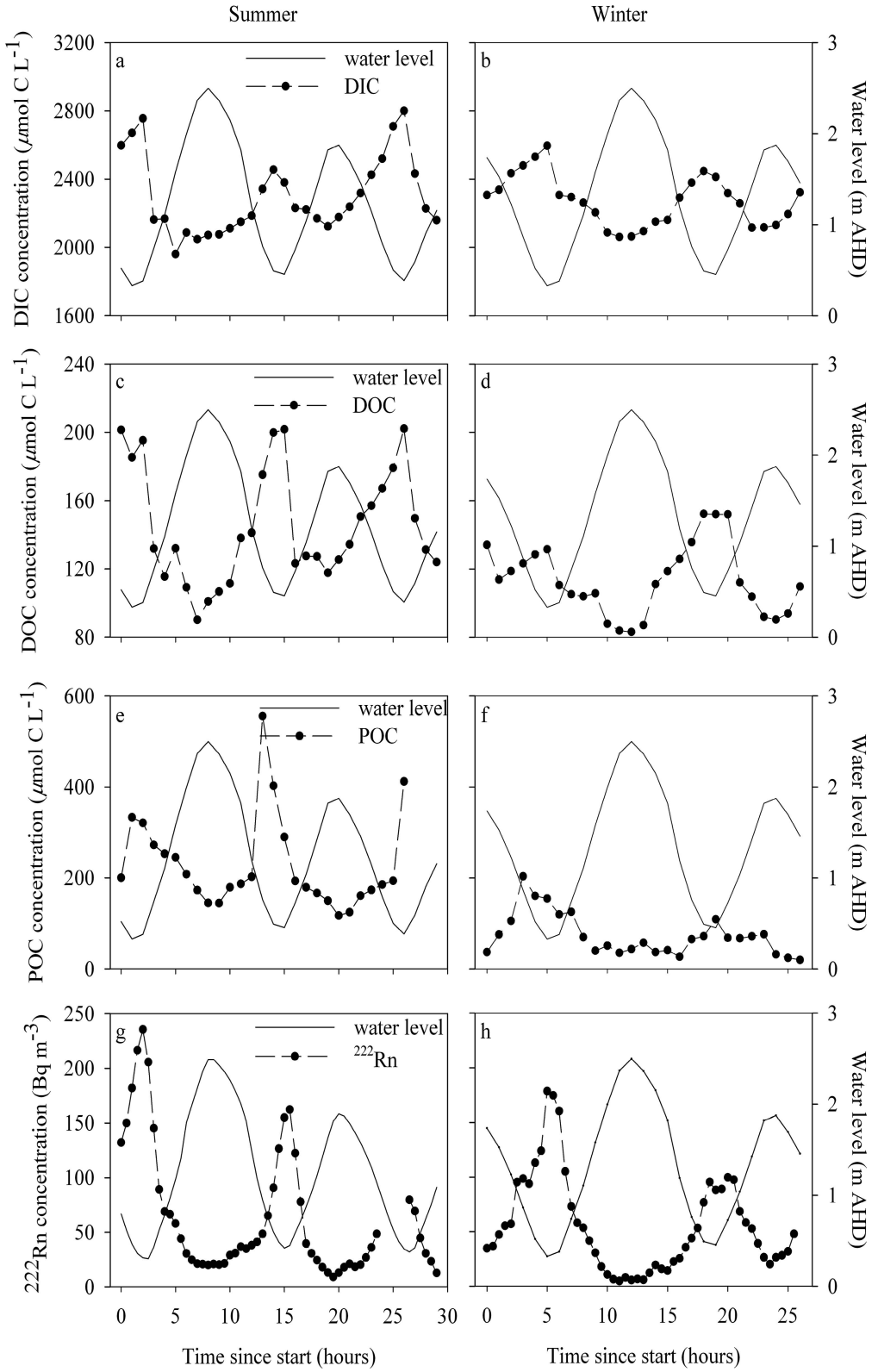

Fig. 2. Tidal variations of water height and DIC concentrations in (a) summer and (b) winter, variations in DOC concentration in (c) summer and (d) winter, variations in POC concentrations in (e) summer and (f) winter, and variations in ^{222}Rn concentrations in (g) summer and (h) winter. (Note: axes are scaled the same for summer and winter for each individual parameter.)

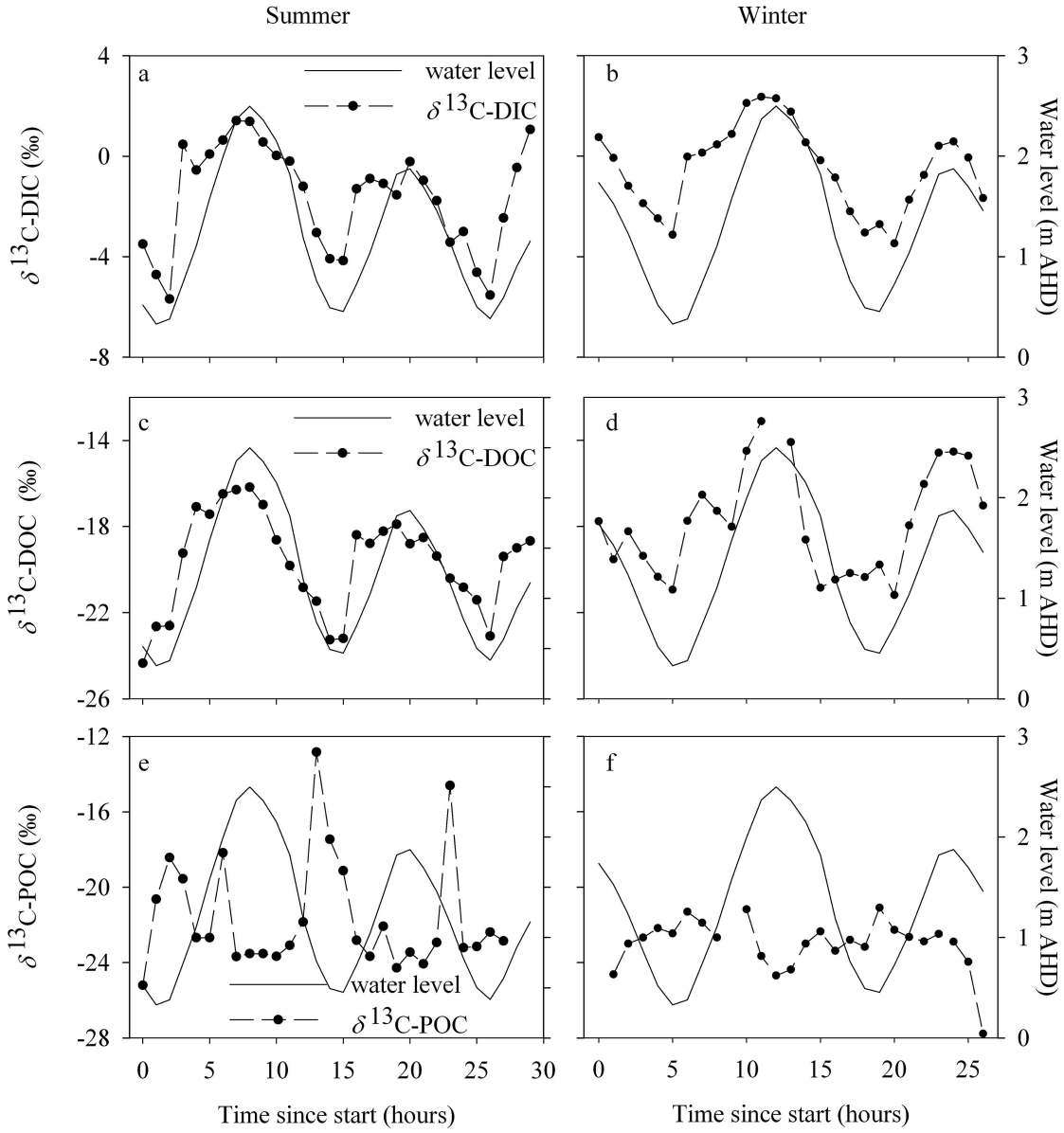

Fig. 3. Variations in creek δ^{13}C-DIC values in (a) summer and (b) winter, variations in creek δ^{13}C-DOC values in (c) summer and (d) winter, and variations in the values of δ^{13}C-POC in the creek in (e) summer and (f) winter. (Note: axes are scaled the same for summer and winter for each individual parameter.)

was exported during each tidal cycle, with rates ranging from 500 to 1700 μmol C m^{-2} h^{-1}. Rates of export of DIC and DOC did not vary substantially between summer and winter large tides, or between the large and small tides during summer. Based on the regression of modeled and measured DIC and DOC concentrations vs. creek volume during ebb tides, groundwater accounted for 89–92% of the DOC export and 93–99% of the DIC export. A similar model was not applied to POC because groundwater exchange is a source of dissolved species only.

Table 2. Dark, light, and net diffusive fluxes of DIC from the lower and upper intertidal areas within the studied mangrove creek catchment. DOC fluxes approached zero in these cores.

	Dark DIC flux (μmol C m^{-2} h^{-1})	Light DIC flux (μmol C m^{-2} h^{-1})	Net DIC flux (μmol C m^{-2} h^{-1})
High intertidal	1056(±62)	921(±310)	993(±121)
Low intertidal	837(±120)	683(±46)	724(±182)

Discussion

Our model used ^{222}Rn to predict the carbon concentration and isotope composition of creek waters if groundwater was the only carbon source to the creek. If modeled and measured values are identical, pore-water exchange would explain 100% of the DIC and DOC exports. Although the relationship between creek DIC and DOC concentrations

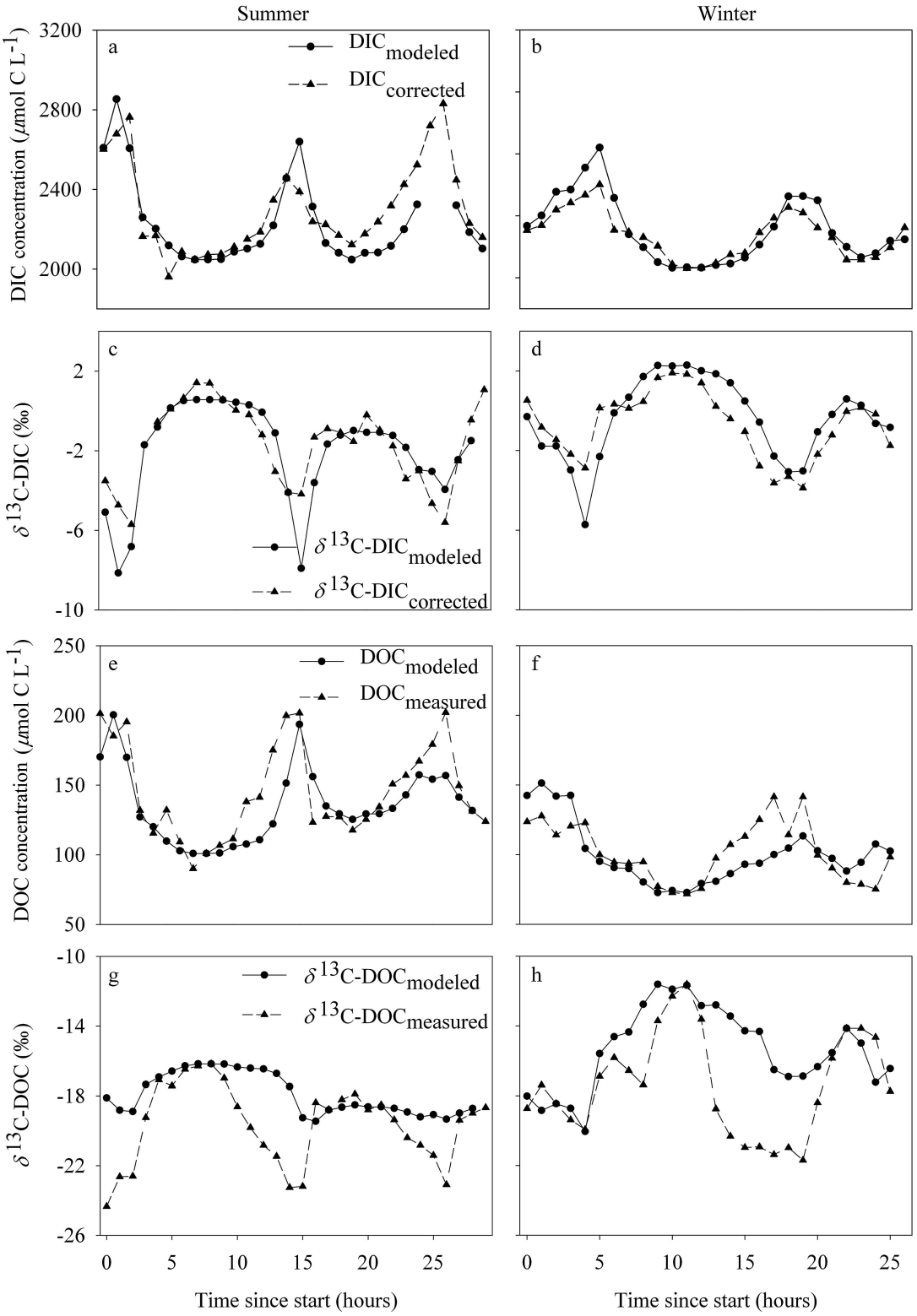

Fig. 4. Modeled and measured concentrations within the mangrove creek of DIC concentration in (a) summer and (b) winter, δ^{13}C-DIC values in (c) summer and (d) winter, DOC concentrations in (e) summer and (f) winter, and δ^{13}C-DOC values in (g) summer and (h) winter. (Note: axes are scaled the same for summer and winter for each individual parameter.)

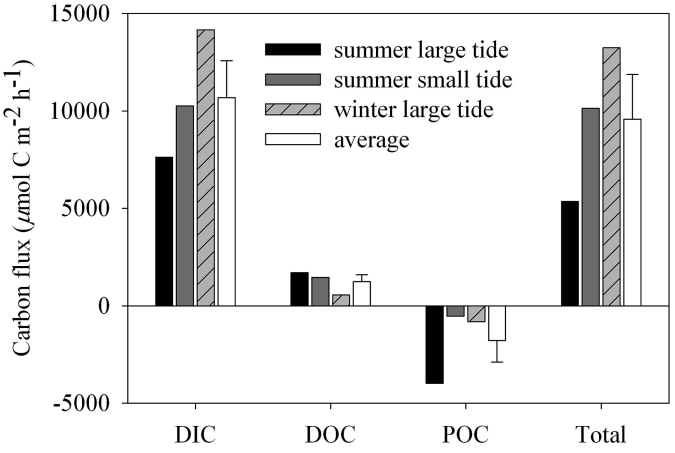

Fig. 5. Carbon export rates for DIC, DOC, POC, and total carbon for each of the individual flood ebb tide cycles. No estimate was available for the small winter tide because of the sampling regime not capturing a consecutive small flood ebb tide cycle.

and ^{222}Rn was clear both in the summer and winter, there are several caveats that need to be considered. Most importantly, our models assume that the groundwater entering the creek is homogenous in DOC and ^{222}Rn concentrations irrespective of tidal level (i.e., we took an average of four groundwater samples along a transect from low tide to high tide level) and that there is no spatial variability in groundwater composition along the creek. This is clearly a simplification (Charette 2007; Dulaiova et al. 2008). However, the low standard error for all variables investigated (less than 5% for DOC and $<$ 20% for ^{222}Rn) and the excellent agreement between measured and modeled values (Fig. 4) suggests that the values used as groundwater end members are reasonable. Further, the small catchment size (0.4 km^2) and short surface water residence time ($\sim$ 1 tidal cycle) likely minimize the influence of any small-scale heterogeneity in groundwater composition. A 3 m deep bore dug in the intertidal area revealed a homogenous muddy sediment column with groundwater flow clearly dominated by crab burrows. Crabs are often seen as mangrove ecosystem engineers (Kristensen 2008) and a number of modeling studies have demonstrated that crab burrows act as preferential groundwater pathways in other mangrove systems (Ridd 1996; Mazda and Ikeda 2006; Xin et al. 2009).

Another potential source of error in our models is using PCO_2 and empirical wind speed models to determine the influence the air–water flux of CO_2 has on both DIC concentrations and δ^{13}C-DIC (for PCO_2 and air–water flux data, *see* Web Appendix, www.aslo.org/lo/toc/vol_58/issue_2/0475a.html). It is well established that using wind-speed parameterizations of piston velocity to calculate air–water CO_2 fluxes introduces uncertainty (Raymond and Cole, 2001; Maher and Eyre 2012), as does calculating PCO_2 from two of the six carbonate system parameters, rather than direct measurements (Zeebe and Wolf-Gladrow 2001). However, the maximum correction associated with the air–sea CO_2 flux term was only $\sim$ 1% (30 μmol C L^{-1}) for DIC concentration and 0.08‰ for δ^{13}C-DIC values (Fig. 6).

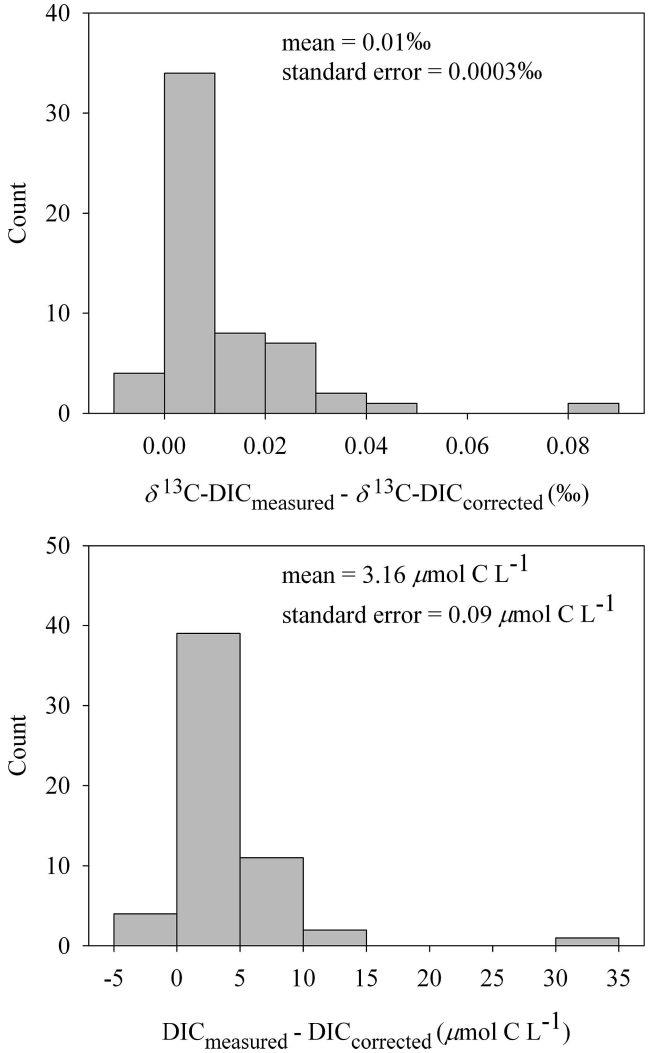

Fig. 6. (top) Histogram of the difference between measured δ^{13}C-DIC and δ^{13}C-DIC values corrected for fractionation due to the calculated air–water CO_2 flux and (bottom) histogram of the difference between measured DIC concentrations and DIC values corrected for changes due to the calculated air–water CO_2 flux.

Therefore, any errors associated with calculations of air–water fluxes have a minor influence on the results.

Sources of DIC, DOC, and POC—Both concentration and δ^{13}C values of the POC, DOC, and DIC pools showed a clear tidal trend (Figs. 2, 3). By plotting the linear regression of 1/concentration against the δ^{13}C values for each pool, the y intercept gives an estimate of the δ^{13}C value "added" carbon (Keeling 1958; Bouillon et al. 2007*b*). When compared to the δ^{13}C value of end members, some insight into the sources can be gained. Values for the added δ^{13}C-DOC ($-$29.2‰ in summer and $-$31.1‰ in winter, Fig. 7) are similar to those of mangrove leaves in the study area (Fig. 8), as has been found previously by Bouillon et al. (2007*b*) in a Tanzanian mangrove system. POC was imported during each tidal cycle (Fig. 5). In spite of the highest concentrations of POC being measured during the ebb tide (Fig. 2), the hourly water fluxes during

this period were low; therefore, the total POC export was low. The high δ^{13}C-POC values measured during the last half of the ebb tides during summer indicate a source other than mangrove detritus is dominant. It is possible that this value is related to resuspension or erosion of sediments colonized by benthic microalgae, which have a similarly enriched δ^{13}C value (~ -18.1‰). The δ^{13}C-POC of this imported organic carbon was -16.3‰ in summer and -22‰ in winter (Fig. 7c). However, there was considerable scatter and lower (yet still significant) coefficient of determination values than for δ^{13}C-DOC and δ^{13}C-DIC. The scatter is likely due to differing sources throughout the tidal cycle. For example, during the start of the flood tide, the source is likely composed of a significant fraction of the POC exported from the mangroves during the previous ebb tide, but as the flood continues, the POC becomes more dominated by estuarine POM (phytoplankton). The summer value likely represents a combination of seagrass, estuarine POM, and mangrove detritus. The winter values are similar to estuarine POM, or possibly a combination of a number of sources (Fig. 8). Seagrasses cover $\sim$ 13% of the adjacent estuary, and the gross primary production of these communities is $\sim$ 4-fold higher in summer (Eyre et al. 2011*b*). The import of seagrass and estuarine POM organic matter to mangroves has been reported in a number of studies previously (Bouillon et al. 2003; Kennedy et al. 2004; Bouillon and Boschker 2006).

The δ^{13}C values for the added DIC were similar between summer (-22.6‰) and winter (-22.3‰) (Fig. 7a), indicating no seasonality in the source of DIC export. Bouillon et al. (2007*b*) found a similar value of -22.4‰, and suggested that DIC export was driven by mineralization of autochthonous (mangrove litter) and allochthonous (estuarine POM and/or seagrass) organic matter, which may be the case in this study (Fig. 8). It should be noted that this value is $\sim$ 8–10‰ more depleted than the measured groundwater δ^{13}C-DIC (Table 1). However, groundwater is also subject to DIC addition through subsurface processes. In the study catchment there are no freshwater inputs, and therefore groundwater circulation is driven by tidal pumping only. If we assume that the composition of water entering the groundwater pool is equivalent to the average composition of creek water during the flood tide, the δ^{13}C-DIC of the DIC produced in the groundwater can be estimated by a mass balance model using groundwater and creek waters as the two end members, using the following equation:

$$\delta^{13}\text{C–DIC}_{\text{gw\_added}} = (\delta^{13}\text{C–DIC}_{\text{gw}} \times \text{DIC}_{\text{gw}}) + \delta^{13}\text{C–DIC}_{\text{input}} \times \text{DIC}_{\text{input}}) / (\text{DIC}_{\text{gw}} - \text{DIC}_{\text{input}}) \quad (7)$$

where δ^{13}C-DIC and DIC are DIC stable carbon isotope ratios and concentration, respectively, and the subscripts gw and input are groundwater and average flood tide concentrations, respectively. The values obtained for DIC added to groundwater during summer and winter are -21.0‰ and -23.1‰, respectively, values very similar to the whole-system added δ^{13}C-DIC values calculated by regression (Fig. 7).

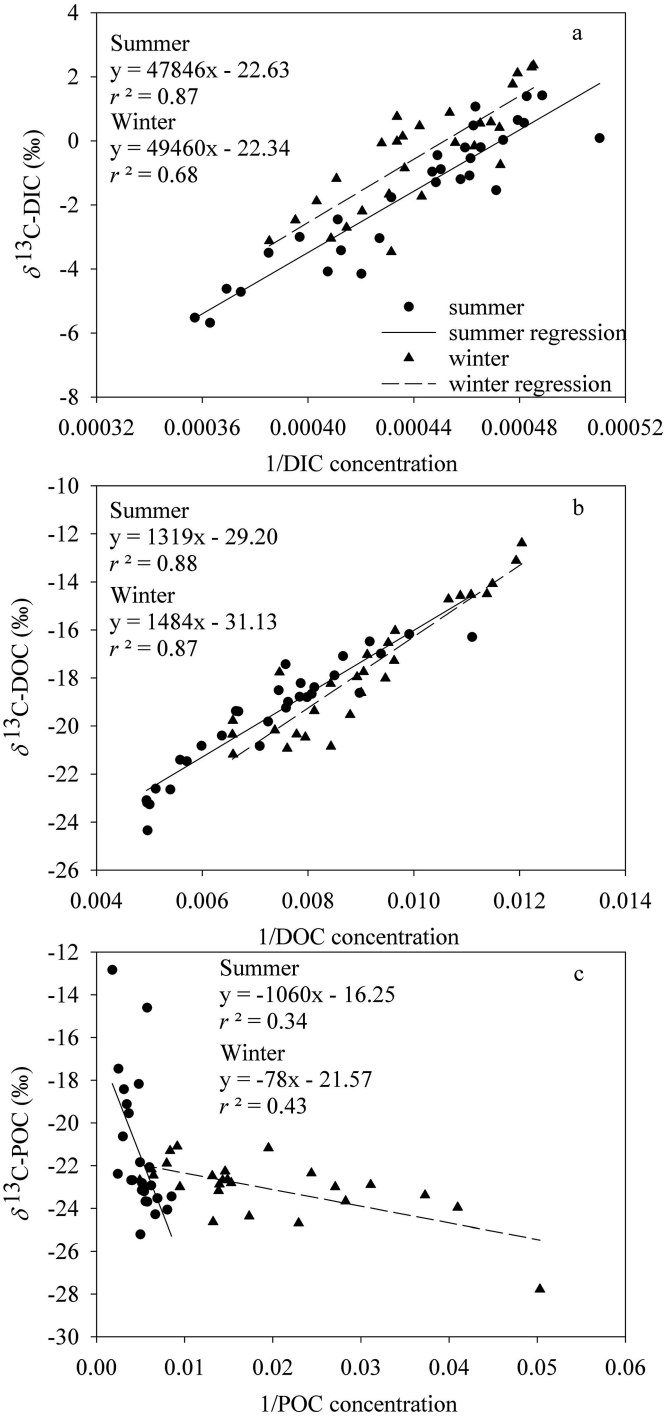

Fig. 7. Regressions of 1/concentration vs. δ^{13}C values for (a) DIC, (b) DOC, and (c) POC. The y intercept of the regression is the estimate of the "added" carbon δ^{13}C value.

Groundwater-derived carbon export—Previous studies have documented an inverse relationship between tidal height and DIC (Borges et al. 2003; Kristensen et al. 2008*b*; Zablocki et al. 2011) and DOC (Lara and Dittmar 1999; Dittmar and Lara 2001) concentrations in mangrove creeks. It has been hypothesized that this tidal variation is driven by the input of groundwater enriched in DIC and DOC during the ebb tide (Dittmar and Lara 2001; Bouillon

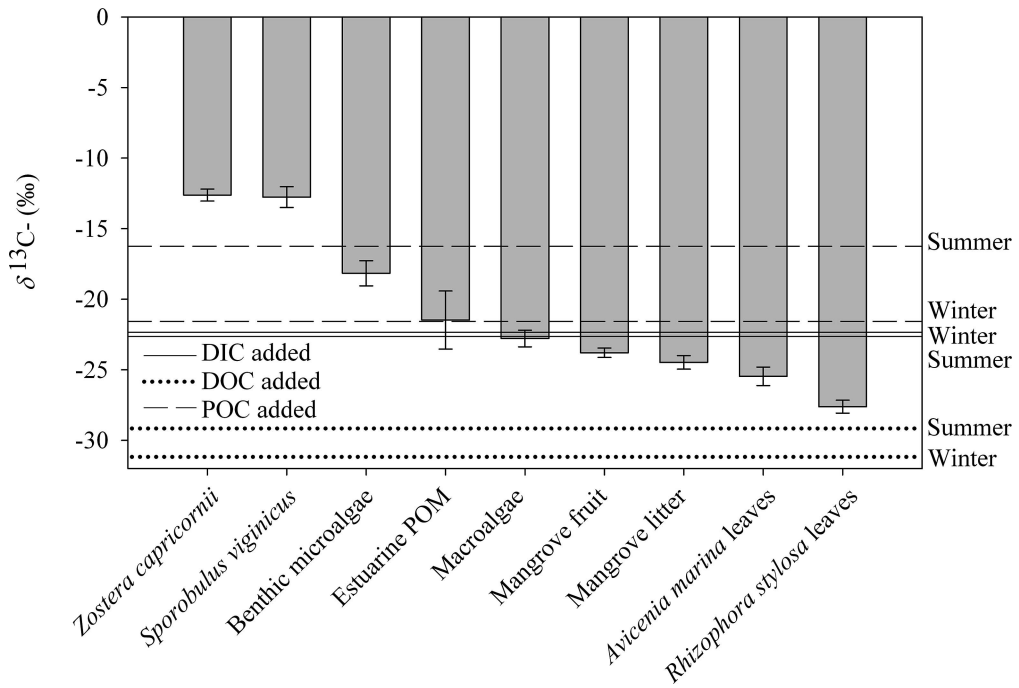

Fig. 8. End-member δ^{13}C values (± 1 SD, n=3 pooled samples) and the summer and winter δ^{13}C values of the added DIC (solid lines), DOC (dotted lines), and POC (dashed lines) obtained from Keeling plots (Fig. 7).

et al. 2007*b*), with connectivity between groundwater and surface water enhanced in mangroves because of the mosaic of macrofauna burrows and organic-rich sediment layers (Ridd 1996; Mazda and Ikeda 2006). We build on these studies by using ^{222}Rn to quantitatively demonstrate the groundwater input. Our observed tidal trends were similar to these previous investigations, and show that groundwater drives the input of DIC and DOC to the creek, and can account for between 89% and 92% of DOC and 93% and 99% of DIC exports.

The coupled ^{222}Rn and δ^{13}C-DIC model further supports the hypothesis that groundwater drives the export of DIC, and that fractionation, uptake, and/or generation of DIC in the surface waters of the creek are a small component of the DIC cycle (Fig. 4). Indeed, the diffusive DIC fluxes measured from both the lower and upper intertidal areas (Table 2) are an order of magnitude lower than whole-system DIC export values (Fig. 5), indicating a relatively small role of surface (diffusive) DIC generation in DIC export from this mangrove system. In contrast, the coupled ^{222}Rn and δ^{13}C-DOC model indicates that there is a significant fractionation of the DOC pool. The modeled results were more enriched than measured results, perhaps as a result of preferential uptake of enriched δ^{13}C-DOC from benthic microalgae, saltmarsh, or imported seagrass, relative to the δ^{13}C-depleted mangrove detritus. If this preferential uptake was the sole driver of DOC fractionation, we would expect a concurrent decrease in measured vs. modeled DOC concentrations, which was not the case (Fig. 4). Another possibility is that the DOC pool was supplemented by depleted δ^{13}C-DOC derived from the surface processes (e.g., leaching from mangrove litter). However, this would also create a discrepancy between modeled and measured concentrations of DOC with measured concentrations increased relative to modeled concentrations. It is therefore likely that a combination of preferential uptake and leaching of depleted δ^{13}C-DOC derived from mangrove detritus was the driver for the observed differences in modeled and measured δ^{13}C-DOC values.

Groundwater-derived DIC, the missing mangrove carbon sink?—In their recent review, Bouillon et al. (2008) found that over 50% of net mangrove production was unaccounted for by estimates of the various carbon sinks, an amount equivalent to ~ 2 g C m^{-2} d^{-1}. A similar global mangrove "missing carbon" value of ~ 2.7 g C m^{-2} d^{-1} was found by Alongi (2009). Previous mangrove carbon budgets have neglected the exchange of DIC, which may lead to significant underestimation of both ecosystem gross primary production and respiration. In addition, neglecting the export of DIC derived from subsurface respiration leads to an overestimation of ecosystem net productivity estimates based on eddy covariance techniques, as long as the CO_2 is fluxed to the atmosphere outside of the measurement "footprint" (Barr et al. 2010) as can occur in many tidal systems.

Although the importance of advective groundwater exchange of both DIC and DOC has been speculated, to our knowledge this is the first study to quantify the importance of this export term through direct measurement of DIC exports and its driver. The DOC export in the present study averaged over the three tidal cycles was ~ 0.3 g C m^{-2} d^{-1}, which is within the range reported for mangrove systems previously (~ 0.02–0.4 g C m^{-2} d^{-2}; Kristensen et al. 2008; Adame and Lovelock 2011). Therefore, the mangrove creek

studied here may be representative of many other mangrove systems. DIC export in the present study ranged from 2.2 to 4.1 g C m^{-2} d^{-1}, and the average over the two summer and one winter tidal cycles was ~ 3 g C m^{-2} d^{-2}. This site-specific value is very similar to the globally averaged mangrove missing carbon (1.9–2.7 g C m^{-2} d^{-2}; Bouillon et al, 2008; Alongi, 2009). Modeling results indicate that tidal pumping was the dominant pathway for carbon export (Fig. 4) and the export of DIC was ~ an order of magnitude higher than DOC export (Fig. 5). This export of DIC may lead to the elevated PCO_2 and high CO_2 fluxes to the atmosphere reported for waters adjacent to mangroves (Borges et al. 2003; Bouillon et al. 2007*a*; Koné and Borges 2008). Further work is needed in a range of mangrove systems from various latitudes, with different geomorphic settings, species compositions, and tidal regimes to constrain the magnitude and drivers of DIC exports, an export term that is potentially important globally. Our results demonstrate that DIC may be the dominant form of carbon exported from mangroves, and that this export is closely related to tidally driven advective groundwater (or porewater) exchange.

Acknowledgments

We thank Matheus Carvalho, who skillfully ran all carbon samples. This project was funded by grants from the Australian Research Council (LP110200975, LP100200732, and DP120101645). Two anonymous reviewers and H. M. Valett provided valuable feedback, which helped improve the manuscript.

References

Adame, M. F., and C. E. Lovelock. 2011. Carbon and nutrient exchange of mangrove forests with the coastal ocean. Hydrobiologia **663:** 23–50, doi:10.1007/s10750-010-0554-7

Alongi, D. M. 2009. The energetics of mangrove forests. Springer.

———, N. A. De Carvalho, A. L. Amaral, A. Da Costa, L. Trott, and F. Tirendi. 2012. Uncoupled surface and belowground respiration in mangroves: Implications for estimates of dissolved inorganic carbon export. Biogeochemistry **109:** 151–162, doi:10.1007/s10533-011-9616-9

Barr, J. G., V. Engel, J. D. Fuentes, J. C. Zieman, T. L. O'Halloran, T. J. Smith, and G. H. Anderson. 2010. Controls on mangrove forest-atmosphere carbon dioxide exchanges in western Everglades National Park. J. Geophys. Res. **115:** G02020, doi:10.1029/2009JG001186

Borges, A. V., S. Djenidi, G. Lacroix, J. Théate, B. Delille, and M. Frankignoulle. 2003. Atmospheric CO_2 flux from mangrove surrounding waters. Geophys. Res. Lett. **30:** 1558, doi:10.1029/2003GL017143

Boto, K. J., and J. T. Wellington. 1988. Seasonal variations in concentrations and fluxes of dissolved organic and inorganic materials in a tropical, tidally-dominated, mangrove waterway. Mar. Ecol. Prog. Ser. **50:** 151–160, doi:10.3354/meps050151

Bouillon, S., and H. T. S. Boschker. 2006. Bacterial carbon sources in coastal sediments: A cross-system analysis on stable isotope data of biomarkers. Biogeosciences **3:** 175–185, doi:10.5194/bg-3-175-2006

———, F. Dahdouh-Guebas, A. V. V. S. Rao, N. Koedam, and F. Dehairs. 2003. Sources of organic carbon in mangrove sediments: Variability and possible ecological implications. Hydrobiologia **495:** 33–39, doi:10.1023/A:1025411506526

———, F. Dehairs, B. Velimirov, G. Abril, and A. V. Borges. 2007*a*. Dynamics of organic and inorganic carbon across contiguous mangrove and seagrass systems (Gazi Bay, Kenya). J. Geophys. Res. **112:** G02018, doi:10.1029/2006JG000325

———, and others. 2007*b*. Importance of intertidal sediment processes and porewater exchange on the water column biogeochemistry in a pristine mangrove creek (Ras Dege, Tanzania). Biogeosciences **4:** 311–322, doi:10.5194/bg-4-311-2007

———, and ———. 2008. Mangrove production and carbon sinks: A revision of global budget estimates. Global Biogeochem. Cycles. **22:** GB2013, doi:10.1029/2007GB00

Burnett, W. C., R. N. Peterson, I. R. Santos, and R. W. Hicks. 2010. Use of automated radon measurements for rapid assessment of groundwater flow into Florida streams. J. Hydrol. **380:** 298–304, doi:10.1016/j.jhydrol.2009.11.005

———, and others. 2006. Quantifying submarine groundwater discharge in the coastal zone via multiple methods. Sci. Total Environ. **367:** 498–543, doi:10.1016/j.scitotenv.2006.05.009

Cai, W.-J., Y. Wang, J. Krest, and W. S. Moore. 2003. The geochemistry of dissolved inorganic carbon in a surficial groundwater aquifer in North Inlet, South Carolina, and the carbon fluxes to the coastal ocean. Geochim. Cosmochim. Acta **67:** 631–637, doi:10.1016/S0016-7037(02)01167-5

Cardenas, M. B., and others. 2010. Linking regional sources and pathways for submarine groundwater discharge at a reef by electrical resistivity tomography, ^{222}Rn, and salinity measurements. Geophys. Res. Lett. **37:** L16401, doi:10.1029/2010GL044066

Charette, M. A. 2007. Hydrologic forcing of submarine groundwater discharge: Insight from a seasonal study of radium isotopes in a groundwater-dominated salt marsh estuary. Limnol. Oceanogr. **52:** 230–239, doi:10.4319/lo.2007.52.1.0230

———, and K. O. Buesseler. 2004. Submarine groundwater discharge of nutrients and copper to an urban subestuary of Chesapeake Bay (Elizabeth River). Limnol. Oceanogr. **49:** 376–385, doi:10.4319/lo.2004.49.2.0376

Cole, J. J., and others. 2007. Plumbing the global carbon cycle: Integrating inland waters into the terrestrial carbon budget. Ecosystems **10:** 171–184, doi:10.1007/s10021-006-9013-8

Cook, P. G., S. Lamontagne, D. Berhane, and J. F. Clark. 2006. Quantifying groundwater discharge to Cockburn River, southeastern Australia, using dissolved gas tracers 222Rn and SF6. Water Resour. Res. **42:** W10411, doi:10.1029/2006WR004921

Dickson, A. G. 1990. Standard potential of the reaction: $AgCl_{(s)} + 1/2\ H_{2(g)} = Ag_{(s)} + HCl_{(aq)}$, and the standard acidity constant of the ion HSO_4^- in synthetic sea water from 273.15 to 318.15 K. J. Chem. Thermodyn. **22:** 113–127, doi:10.1016/0021-9614(90)90074-Z

Dittmar, T., N. Hertkorn, G. Kattner, and R. J. Lara. 2006. Mangroves, a major source of dissolved organic carbon to the oceans. Global Biogeochem. Cycles **20:** GB1012, doi:10.1029/2005GB002570

———, and R. J. Lara. 2001. Driving forces behind nutrient and organic matter dynamics in a mangrove tidal creek in North Brazil. Estuar. Coast. Shelf Sci. **52:** 249–259, doi:10.1006/ecss.2000.0743

Donato, D. C., J. B. Kauffman, D. Murdiyarso, S. Kurnianto, M. Stidham, and M. Kanninen. 2011. Mangroves among the most carbon-rich forests in the tropics. Nat. Geosci. **4:** 293–297, doi:10.1038/ngeo1123

Dulaiova, H., M. E. Gonneea, P. B. Henderson, and M. A. Charette. 2008. Geochemical and physical sources of radon variation in a subterranean estuary—implications for groundwater radon activities in submarine groundwater discharge studies. Mar. Chem. **110:** 120–127, doi:10.1016/j.marchem.2008.02.011

———, R. Peterson, W. Burnett, and D. Lane-Smith. 2005. A multi-detector continuous monitor for assessment of ^{222}Rn in the coastal ocean. J. Radioanal. Nucl. Chem. **263:** 361–365.

Eyre, B. D., A. J. P. Ferguson, A. Webb, D. Maher, and J. M. Oakes. 2011*a*. Denitrification, N-fixation and nitrogen and phosphorus fluxes in different benthic habitats and their contribution to the nitrogen and phosphorus budgets of a shallow oligotrophic sub-tropical coastal system (southern Moreton Bay, Australia). Biogeochemistry **102:** 111–133, doi:10.1007/s10533-010-9425-6

———, ———, A. P. Webb, D. Maher, and J. M. Oakes. 2011*b*. Metabolism of different benthic habitats and their contribution to the carbon budget of a shallow oligotrophic subtropical coastal system. Biogeochemistry **103:** 87–110, doi:10.1007/s10533-010-9424-7

Jennerjahn, T. C., and V. Ittekkot. 2002. Relevance of mangroves for the production and deposition of organic matter along tropical continental margins. Naturwissenschaften **89:** 23–30, doi:10.1007/s00114-001-0283-x

Keeling, C. D. 1958. The concentration and isotopic abundances of atmospheric carbon dioxide in rural areas. Geochim. Cosmochim. Acta **13:** 322–334, doi:10.1016/0016-7037(58)90033-4

Kennedy, H., E. Gacia, D. P. Kennedy, S. Papadimitriou, and C. M. Duarte. 2004. Organic carbon sources to SE Asian coastal sediments. Estuar. Coast. Shelf Sci. **60:** 59–68, doi:10.1016/j.ecss.2003.11.019

Koné, Y. J. M., and A. V. Borges. 2008. Dissolved inorganic carbon dynamics in the waters surrounding forested mangroves of the Ca Mau Province (Vietnam). Estuar. Coast. Shelf Sci. **77:** 409–421, doi:10.1016/j.ecss.2007.10.001

Kristensen, E. 2008. Mangrove crabs as ecosystem engineers; with emphasis on sediment processes. J. Sea Res. **59:** 30–43, doi:10.1016/j.seares.2007.05.004

———, S. Bouillon, T. Dittmar, and C. Marchand. 2008*a*. Organic carbon dynamics in mangrove ecosystems: A review. Aquat. Bot. **89:** 201–219, doi:10.1016/j.aquabot.2007.12.005

———, M. R. Flindt, S. Ulomi, A. V. Borges, G. Abril, and S. Bouillon. 2008*b*. Emission of CO_2 and CH_4 to the atmosphere by sediments and open waters in two Tanzanian mangrove forests. Mar. Ecol. Prog. Ser. **370:** 53–67, doi:10.3354/meps07642

Lara, R. J., and T. Dittmar. 1999. Nutrient dynamics in a mangrove creek (North Brazil) during the dry season. Mangroves Salt Marshes **3:** 185–195, doi:10.1023/A:1009903824243

Lewis, E., and D. W. R. Wallace. 1998. Program developed for CO2 system calculations [Internet]. Carbon Dioxide Information Analysis Center, Oak Ridge National Laboratory, US Department of Energy [accessed 2012 February 02]. Available from http://cdiac.ornl.gov/oceans/co2rprt.html

Lim, S. 2006. Fiddler crab burrow morphology: How do burrow dimensions and bioturbative activities compare in sympatric populations of *Uca vocans* (Linnaeus, 1758) and *U. annulipes* (H. Milne Edwards, 1837)? Crustaceana **79:** 525–540, doi:10.1163/156854006777584241

Maher, D., and B. D. Eyre. 2010. Benthic fluxes of dissolved organic carbon in three temperate Australian estuaries: Implications for global estimates of benthic DOC fluxes. J. Geophys. Res. **115:** G04039, doi:10.1029/2010JG001433

———, and ———. 2011*a*. Benthic carbon metabolism in South-East Australian estuaries: Habitat importance, driving forces and application of artificial neural network models. Mar. Ecol. Prog. Ser. **439:** 97–115, doi:10.3354/meps09336

———, and ———. 2011*b*. Insights into estuarine benthic dissolved organic carbon (DOC) dynamics using δ^{13}C-DOC values, phospholipid fatty acids and dissolved organic nutrient fluxes. Geochim. Cosmochim. Acta **75:** 1889–1902, doi:10.1016/j.gca.2011.01.007

———, and ———. 2012. Carbon budgets for three autotrophic Australian estuaries: Implications for global estimates of the coastal air-water CO_2 flux. Global Biogeochem. Cycles **26:** GB1032, doi:10.1029/2011GB004075

Mazda, Y., and Y. Ikeda. 2006. Behavior of the groundwater in a riverine-type mangrove forest. Wetlands Ecol. Manage. **14:** 477–488.

Meziane, T., F. D'Agata, and S. Y. Lee. 2006. Fate of mangrove organic matter along a subtropical estuary: Small-scale exportation and contribution to the food of crab communities. Mar. Ecol. Prog. Ser. **312:** 15–27, doi:10.3354/meps312015

Millero, F. J., T. B. Graham, F. Huang, H. Bustos-Serrano, and D. Pierrot. 2006. Dissociation constants of carbonic acid in seawater as a function of salinity and temperature. Mar. Chem. **100:** 80–94, doi:10.1016/j.marchem.2005.12.001

Miyajima, T., Y. Tsuboi, Y. Tanaka, and I. Koike. 2009. Export of inorganic carbon from two Southeast Asian mangrove forests to adjacent estuaries as estimated by the stable isotope composition of dissolved inorganic carbon. J. Geophys. Res. **114:** G01024, doi:10.1029/2008JG000861

Peterson, B., B. Fry, M. Hullar, S. Saupe, and R. Wright. 1994. The distribution and stable carbon isotopic composition of dissolved organic carbon in estuaries. Estuaries **17:** 111–121, doi:10.2307/1352560

Peterson, R. N., I. R. Santos, and W. C. Burnett. 2010. Evaluating groundwater discharge to tidal rivers based on a Rn-222 time-series approach. Estuar. Coast. Shelf Sci. **86:** 165–178, doi:10.1016/j.ecss.2009.10.022

Raymond, P. A., and J. J. Cole. 2001. Gas exchange in rivers and estuaries: Choosing a gas transfer velocity. Estuaries **24:** 312–317, doi:10.2307/1352954

Ridd, P. V. 1996. Flow through animal burrows in mangrove creeks. Estuar. Coast. Shelf Sci. **43:** 617–625, doi:10.1006/ecss.1996.0091

Robeson, S. M., and K. A. Shein. 1997. Spatial coherence and decay of wind speed and power in the north-central United States. Phys. Geogr. **18:** 479–495.

Robinson, C., L. Li, and H. Prommer. 2007. Tide-induced recirculation across the aquifer-ocean interface. Water Resour. Res. **43:** W07428, doi:10.1029/2006WR005679

Santos, I. R., W. C. Burnett, T. Dittmar, I. G. N. A. Suryaputra, and J. Chanton. 2009. Tidal pumping drives nutrient and dissolved organic matter dynamics in a Gulf of Mexico subterranean estuary. Geochim. Cosmochim. Acta **73:** 1325–1339, doi:10.1016/j.gca.2008.11.029

———, P. L. M. Cook, L. Rogers, J. de Weys, and B. D. Eyre. 2012*a*. The "salt wedge pump": Convection-driven porewater exchange as a source of dissolved organic and inorganic carbon and nitrogen to an estuary. Limnol. Oceanogr. **57:** 1415–1426, doi:10.4319/lo.2012.57.5.1415

———, D. T. Maher, and B. D. Eyre. 2012*b*. Coupling automated radon and carbon dioxide measurements in coastal waters. Environ. Sci. Technol. **46:** 7685–7691, doi:10.1021/es301961b

Schmidt, A., J. J. Gibson, I. R. Santos, M. Schubert, K. Tattrie, and H. Weiss. 2010. The contribution of groundwater discharge to the overall water budget of two typical Boreal lakes in Alberta/Canada estimated from a radon mass balance. Hydrol. Earth Syst. Sci. **14:** 79–89, doi:10.5194/hess-14-79-2010

Stieglitz, T., P. G. Cook, and W. C. Burnett. 2010. Inferring coastal processes from regional-scale mapping of ^{222}Radon and salinity: Examples from the Great Barrier Reef, Australia. J. Environ. Radioact. **101:** 544–552, doi:10.1016/j.jenvrad.2009.11.012

St-Jean, G. 2003. Automated quantitative and isotopic (^{13}C) analysis of dissolved inorganic carbon and dissolved organic carbon in continuous-flow using a total organic carbon analyser. Rapid Commun. Mass Spectrom. **17:** 419–428.

Wanninkhof, R. 1992. Relationship between wind speed and gas exchange over the ocean. J. Geophys. Res. **97:** 7373–7382, doi:10.1029/92JC00188

Xin, P., G. Jin, L. Li, and D. A. Barry. 2009. Effects of crab burrows on pore water flows in salt marshes. Adv. Water Resour. **32:** 439–449, doi:10.1016/j.advwatres.2008.12.008

Yuan, L.-R., P. Xin, J. Kong, L. Li, and D. Lockington. 2011. A coupled model for simulating surface water and groundwater interactions in coastal wetlands. Hydrol. Processes **25:** 3533–3546, doi:10.1002/hyp.8079

Zablocki, J. A., A. J. Andersson, and N. R. Bates. 2011. Diel aquatic CO_2 system dynamics of a Bermudian mangrove environment. Aquat. Geochem. **17:** 841–859, doi:10.1007/s10498-011-9142-3

Zeebe, R. E., and D. Wolf-Gladrow [Eds.]. 2001. CO_2 in seawater: Equilibrium, kinetics, isotopes. Elsevier Science B.V.

Zhang, J., P. D. Quay, and D. O. Wilbur. 1995. Carbon isotope fractionation during gas-water exchange and dissolution of CO_2. Geochim. Cosmochim. Acta **59:** 107–114, doi:10.1016/0016-7037(95)91550-D

Associate editor: H. Maurice Valett

Received: 27 April 2012
Accepted: 20 October 2012
Amended: 28 October 2012